Published in final edited form as:
IEEE Trans Biomed Eng. 2005 August ; 52(8): 1470–1477.

An Array of Microactuated Microelectrodes for Monitoring Single-Neuronal Activity in Rodents

Jit Muthuswamy, **Murat Okandan**, **Aaron Gilletti**, **Michael S. Baker**, and **Tilak Jain**
Harrington Department of Bioengineering, ECG 334, P.O. Box 879709, Arizona State University, Tempe, AZ 85287-9709 USA (e-mail: jit@asu.edu).

MEMS Science and Technology, Sandia National Laboratories, Albuquerque, NM 87185 USA.

Harrington Department of Bioengineering, ECG 334, Arizona State University, Tempe, AZ 85287-9709 USA.

Abstract

Arrays of microelectrodes used for monitoring single-and multi-neuronal action potentials often fail to record from the same population of neurons over a period of time for several technical and biological reasons. We report here a novel Neural Probe chip with a 3-channel microactuated microelectrode array that will enable precise repositioning of the individual microelectrodes within the brain tissue after implantation. Thermal microactuators and associated microelectrodes in the Neural Probe chip are microfabricated using the Sandia's Ultraplanar Multi-level MEMS Technology (SUMMiTV) process, a 5-layer polysilicon microma-chining technology of the Sandia National labs, Albuquerque, NM. The Neural Probe chip enables precise bi-directional positioning of the microelectrodes in the brain with a step resolution in the order of 8.8μm. The thermal microactuators allow for a linear translation of the microelectrodes of up to 5 mm in either direction making it suitable for positioning microelectrodes in deep structures of a rodent brain. The overall translation in either direction was reduced to approximately 2 mm after insulation of the microelectrodes with epoxy for monitoring multi-unit activity. Single unit recordings were obtained from the somatosensory cortex of adult rats over a period of three days demonstrating the feasibility of this technology. Further optimization of the microelectrode insulation and chip packaging will be necessary before this technology can be validated in chronic experiments.

Index Terms

Action-potentials; BioMEMS; brain-implants; microactuators; neuro-prosthesis

I. Introduction

ELECTRICAL activity from single neurons has been critical in enabling our understanding of function, dysfunction and restoration of neuronal function. Sequentially recording single-neuronal electrical activity enables us to understand the behavior of different neurons and the interactions among them. However, information on the emergent properties of assemblies of neurons is lost. Therefore, over the last couple of decades, technology for neuronal monitoring has been focused on monitoring from a population of neurons simultaneously using multi-channel microelectrodes. The early, fixed electrode arrays were produced by photolithography

Correspondence to: Jit Muthuswamy.

This work was supported in part by the Whitaker foundation and in part by the National Institutes of Health (NIH) under Grant R21 NS41681.

[1]–[10]. The inability to independently position each electrode of the array remains one of the shortcomings of this type of fixed electrode arrays. This constrains the user to optimally position the entire array of electrodes to maximize the number of neurons of interest that need to be monitored. Besides this lack of spatial precision, it is common to lose electrical contact with neurons due to either a gradual drift in the microelectrode or micromotion of brain tissue during chronic measurements in freely moving animals. Electrical contact with neurons could also be lost due to impalement by the microelectrode or neuronal death due to pathological reasons. The above limitations on the fixed electrode arrays have made electrophysiological recordings over long periods of time with implanted fixed microelectrode arrays very difficult and cumbersome.

The Reitboeck method of multi-electrode recording [11]–[14], now commercially produced by Uwe Thomas Recording (Marburg, Germany), allowed for independent movement of each electrode in the z-dimension. The individual electrodes could also be arranged in a choice of spatial patterns in X-Y dimensions. The microdrives are powered by dc micromotors that can position quartz-platinum microelectrodes in 1 μm steps. In addition, the motors allowed penetrations of dura and recordings from brain regions that were as deep as 20 mm. Frederick Haer and Co. (Bowdoinham, ME) and Alpha Omega Engineering (Nazareth, Israel) have also developed similar microelectrode positioning systems all of which can only be used when the animal's head is restrained. The size and weight of the above devices make it unsuitable for recording from awake, behaving animals that are moving around. Several individual investigators have also developed microdrives that can be used to move microelectrodes manually [15]–[17]. A chronic microdrive system developed by D. Kopf Instruments (Tujunga, CA) provides independent adjustments of 5 to 10 μm in each channel with a total electrode movement of 7.5 mm. However, the *manual* adjustment of microelectrodes in these devices makes them less reliable and the positioning less reproducible. More recently, a miniature motor-based microelectrode positioning technology using commercially available micromotors has been reported [18].

Therefore, while there is a critical need for a microdrive technology to enable precise positioning of microelectrodes in an array, a technology for doing this is not readily available. We report here a novel microfabricated microactuator technology that will enable independent precise positioning of the individual microelectrodes in an array. Also, unlike a regular hydraulic drive, the light and compact nature of this technology will enable it to be implanted and carried by an unrestrained animal to allow tests in a wider range of behavioral tasks. In addition, the process of microfabrication lends itself readily to future integration with signal conditioning circuitry on the same substrate.

II. Materials and Methods

A. Principle

In this proposed design, the actuator works by getting two slightly angled sets of polysilicon beams as shown in Fig. 1 to buckle in plane due to the applied current and following increase in temperature of the beams. The actuator beams heat up to several hundred degrees Celsius, however, since the thermal masses are so small and conduction is so quick, none of the structures around are at a significantly elevated temperature (a rise in temperature of several degrees celcius is observed only within several microns in the vicinity) during the optimized driving of the actuator [19]. These actuators are coupled to a ratcheting system that drives a center shuttle up or down, depending on which set of actuators is being activated. While the up-drive is engaged (to pull the shuttle up), a set of ratchet pawls for the down-drive are pulled away and disengaged from the shuttle to allow free motion. At the end of the actuation cycle, both sets of pawls are in place, therefore preventing the shuttle from moving in either direction.

The unit step motion is determined by the stroke of the actuator and the separation of the ratchet teeth on the shuttle.

B. Design

Actuation and passive locking of the shuttles (or microelectrodes) is accomplished by the use of linear thermal actuators [20]–[22] attached to a ratchet system. This drive mechanism allows for unlocking, actuation in both directions, and locking of the structure with only four relatively simple drive signals and a ground. The design layout of the microelectrode and the associated microactuators is shown in Fig. 2.

The complete actuator is shown in Fig. 3(a), and can be broken down into two nearly identical parts. Each part contains a single drive actuator connected to a ratchet pawl that indexes the shuttle forward one ratchet tooth per actuation cycle, with an anchored counter-translation latch that prevents motion in the opposite direction, as shown in Fig. 3(b). The ratchet pawl and counter-translation latch are both coupled to an actuator that can disengage them from the shuttle ratchet teeth.

The two parts of the complete drive mechanism are then configured in opposite directions such that one will be used to extend the shuttle and the other used to retract. Two sets of ratchet teeth are attached to the probe and oriented for each of the two directions using the multiple polysilicon layers available in the Sandia National Laboratories[1] SUMMiTV surface micromachining process, with one set configured using the lower layer (*Poly12* laminate), and the second set using the middle layer (*Poly3*).

Because the ratchets and drive teeth are facing opposite directions for each of the two parts of the complete design, the probe is completely constrained and locked into position when no power is applied to the mechanism. To extend the probe, the ratchet pawl and counter-translation latch used to control motion in the retract direction must be disengaged from the probe ratchet teeth as shown in Fig. 4. This allows the drive actuator in the extend direction to operate and translate the probe. Retracting the probe requires the same signal logic applied to the opposite portions of the drive mechanism.

C. Fabrication

These devices were fabricated using the Sandia National Laboratories SUMMiTV technology illustrated in Fig. 5. A brief description of the process is given here, more information on the SUMMiTV technology can be found elsewhere [23].

Six-inch silicon wafers are used as starting material. Insulation layers of 0.6 μm oxide and 0.8 μm low-stress nitride are grown and deposited, respectively. Cuts performed in this layer provide electrical contacts to the substrate. The first polysilicon layer (*Poly0*, 0.3 μm thick, 28 Ω/square) is then deposited and patterned. This layer is used primarily for ground planes and signal routing. A 2-μm -thick sacrificial oxide layer (*sacox1*) is then deposited. In two etch steps, dimples (partially etched through the oxide) and through holes are then defined. Dimples are used to prevent stiction and reduce contact area between mechanical layers. Next, the *Poly1* layer (1μm thick, 23Ω/square) is deposited and partially patterned. An isotropic oxide etch, followed by a conformal (sacrificial) 0.5 μm thick oxide (*sacox2*) deposition defines the separation between the pins and the hubs. Remaining *Poly1* structures are defined in the next etch step. The *Poly2* deposition (1.5 μm thick, 22 Ω/square) forms the captive mechanical elements (pins, hubs, etc.) when the polysilicon conformally fills in the open areas. Structures

[1]Sandia is a multiprogram laboratory operated by Sandia Corporation, a Lock-heed Martin Company, for the United States Department of Energy's National Nuclear Security Administration under contract DE-AC04-94AL85000.

and etch release holes are defined in the polysilicon etching step. *Sacox3* is then deposited and chemical-mechanical polished (CMP) to 2 μm thickness over the *Poly2* layer. Dimples are defined by etching through the oxide and backfilling with a 0.3 μm thick oxide deposition. Through holes are defined by the next oxide etch step. The *Poly3* layer (2.25 μm thick, 8 Ω/square) is then deposited and patterned. *Sacox4* and *Poly4* layers follow the same steps as *Sacox3* and *Poly3*. Spring-type leads make electrical contact from stationary bond pads to the moving microelectrodes as shown in Fig. 6(a). Parts are then separated, released in an HF solution, super critical CO_2 dried and vapor phase SAM (self assembling monolayer) coated. Released parts are attached and wire-bonded in modified DIP's or other packages that have one edge open to allow extension of the neural probe. An SEM of the lower edge of a chip with the three microelectrodes is shown in Fig. 6(b). The current packaging using DIP sockets results in a final dimension of approximately 15 × 25 mm.

D. Insulation

The Neural probe chip was mounted on a hydraulic micromanipulator with the microelectrodes extended up to approximately 3 mm. A small beaker filled with biocompatible epoxy (48-1696, P.D. George Co., St. Loius, MO) was placed under the chip. The microelectrode was steadily dipped into the epoxy till the edge of the PC board, ensuring no epoxy stuck to the surface of the chip itself. The chip was then pulled out of the epoxy beaker at the same rate. To partially cure the epoxy the chip and the microelectrodes were baked in the oven at 99 °C for 30 min. The Neural probe chip was again mounted on the hydraulic micro-manipulator with the microelectrode tips facing down. A beaker filled with dichloro-methane was placed below the microelectrode tips. Dichloro-methane was used to etch the epoxy present on the tip, exposing the conductive core. The microelectrode was steadily lowered till the tips were barely touching the surface of the dichloro-methane (this was done visually by adjusting a Leica GZ6 stereo-microscope horizontally). The microelectrode was then dipped inside the dichloro-methane until impedance of approximately 1–2 MΩ was obtained at 1 kHz. Finally, the chip was baked in the oven at 200 °C to fully cure the epoxy insulation. Upon examination under the microscope, approximately 50 μm from the tapered tip of the microelectrode was etched of the epoxy using this procedure. The Neural Probe chip housing the microactuator and the microelectrode after insulation and establishing electrical contact is shown in Fig. 7.

E. Electrical Impedance Test

The chip was mounted on a hydraulic micro-manipulator with the microelectrode tips facing down. A small beaker filled with Phosphate buffered Saline (PBS) was placed below the chip. A 3-electrode impedance test was performed using an electro-chemical workstation (Model 660A CH Instruments, TX). A platinum counter electrode, a silver reference electrode and the polysilicon microelectrode as the working electrode were used. The counter and the reference electrodes were positioned inside the beaker filled with PBS, ensuring no direct contact between them. The polysilicon microelectrode tip was then lowered till the microelectrode was at least 1 mm inside the solution. An ac impedance test was run from 0.1 Hz to 100 KHz at a voltage of 0.05 V (as shown in Fig. 8).

F. Surgery and Implantation

Male Sprague Dawley rats of approximately 250–300 grams (g) were used. All surgical procedures were carried out with the approval of the Institute Animal Care and Use Committee (IACUC) of Arizona State University, Tempe. The experiments were preformed in accordance with the National Institute of Health (NIH) guide for the care and use of laboratory animals (NIH publications no. 80-23) revised 1996. All efforts were made to minimize animal suffering and to use only the number of animals necessary to produce reliable scientific data, and to utilize alternatives to in-vivo techniques, if available.

Each animal was initially anesthetized using 1 ml/kg of anesthetic cocktail composed of 100 mg/mlKetamine, 20 mg/ml Xylazine, 10 mg/ml Acepromazine mixed with sterilewater. The rat was periodically checked for depth of anesthesia by observing responses to a tail-pinch, and a maintenance dose of 0.5 ml/kg of the cocktailwas administered when necessary. After being anesthetized the animal was then prepared for surgery by shaving the head starting from right in front of the eyes to the base of the neck. After shaving was complete, alcohol and betadine were used to sterilize the surgical area. Askin incisionwas done to expose the skull. A 1/16-in hand drill was used to bore a hole 1 mm posterior and 3 mm lateral to the bregma. Once the implant site was cleared of bone chips, the dura was cut using a 25-gauge needle and the brainwas exposed. The electrodewas then implanted into the somatosensory cortex. The ground wirewas wrapped around a metal screw implanted in the skull in the vicinity of the craniotomy. After implantation, the site was covered with gel foam. Dental acrylic was used to anchor the Neural probe chip to the skull after completely drying the skull surface. Skin was sutured around the Neural probe chip and an antibiotic cream was administered to reduce the chances of infection at the surgery site.

G. Actuation

The individual microactuators in the Neural Probe chip are controlled by four input signals and a ground. The four input signals are “Release-down” and “Release-up” (that release the locks for downward and upward movement of the microelectrode, respectively), “Move-down” and “Move-up” (that activates two other microactuators to move the microelectrode down or up, respectively). For instance, downward movement is accomplished by activating “Release-down” first to release the ratchet pawls and counter translation latch holding the microelectrode and then activating “Move-down” while both “Release-up” and “Move-up” are in the idle state (de-activated). The microelectrode moves down by one step each time “Move-down” is activated.

H. Data Acquisition and Analysis

Multi-unit data was acquired on day 2 and day 3 using a 32-channel neural data acquisition system (TDT Inc., Boca Raton, FL) after the post-operative recovery of animals. Signals were then sorted using principal component analysis and analyzed using the software in Plexon multi-channel neural acquisition systems (Plexon Inc., Dallas, TX). Matlab was used to calculate the signal-to-noise ratio (SNR). A threshold is set at three times the standard deviation of the signal. Peaks that cross this threshold are defined as signal and all other signal is considered as noise. Signal amplitudes are squared and divided by the number of peaks that cross the threshold. Noise is treated in similar fashion, and the logarithm of the ratio of the signal-to-noise is then calculated as a measure of SNR.

III. Results

Five different thermal microactuators have been bench-tested so far and one of them has been implanted in rat brain for 3 days. The two actuators that are used to disengage the ratchet pawl and counter-translation latch are connected in parallel on the MEMS die, and together require approximately 10 V and 35 mA of dc power to operate. While this power is applied to hold open these latches, the drive actuator can then be repeatedly actuated with a series of square pulses. Each pulse requires approximately 10 V and 18 mA to ratchet over one tooth, resulting in a linear displacement of 8.8 μm per actuation. Alternately, the two actuators used to control the ratchet pawls can be activated just before activation of the drive actuator using waveforms similar to the one shown in Fig. 6(c).We have found that in most cases the actuators that release the ratchet pawls [labeled as “Release-down” in Fig. 6(c)] can be activated approximately 25 ms before the activation of the drive actuator [labeled as “Move-down” in Fig. 6(c)] and

deactivated any-time after the deactivation of the drive actuator for successful translation of the microprobe.

The total linear translation of the polysilicon microelectrode in the brain before insulation with epoxy was approximately 5 mm. However, after insulating approximately 3 mm of the microelectrode from the tip, the total linear translation achievable dropped to approximately 2 mm due to masking of the teeth in the microelectrode by the epoxy coating. The force generated by the thermal microactuator has been estimated using finite element models to be in the order of several hundreds of micro-Newtons in a previous study [19] and was found to be sufficient to move the polysilicon microelectrodes in the brain in both directions after implantation. The electrical impedance spectra of the epoxy insulated polysilicon microelectrode over a period of 6 days in saline as shown in Fig. 8, indicates no significant change in the magnitude of the impedance over the first two days (approximately 1 MΩ at 1 kHz). By day 6, the magnitude of the impedance has dropped to approximately 100 kΩ at 1 kHz. The charge-transfer properties and stability of the epoxy insulated polysilicon microelectrode is discussed in greater detail in our previous study [24].

Multi-unit activity was obtained from 2 channels for 3 days with SNR's in the range of 25–30 dB and maximum peak-to-peak amplitude of action potentials in the range of 400–900 μV as shown in Fig. 9. We failed to obtain multi-unit activity in the third channel due to breakage in the channel-3 microelectrode during implantation. Multi-unit activity from channel 1 on day 2 is shown in Fig. 9(a). The insets in the figures show multiple occurrences of two isolated single units. On day 2, we failed to record single units from the microelectrode corresponding to channel 2 as shown in Fig. 9(b). We then moved the microelectrode of channel 2 by an additional 90 μm (by pulsing the actuators for releasing the ratchet-pawls and the drive actuators with 10 rectangular pulses each) to record from a different ensemble of neurons within the somatosensory cortex as shown in Fig. 9(b). We continued to get multi-unit data from both channels on day 3. However, activity in channel 1 was subdued on day 3 as shown in Fig. 9 (c). Multiple occurrences of one of the single units are shown in the inset of Fig. 9(c). At least two single units were isolated in channel 2 on day 3 as shown in the inset of Fig. 9(d).

IV. Discussion

The device reported here addresses a critical need for a technology that will enable repositioning of neural microelectrodes after implantation in the brain. In this regard, our current Neural probe chip with thermal microactuators to move the microelectrodes improves upon previous technologies reported by us and several other groups in several ways as discussed below. None of the previous actuator technologies reported by others [11]–[13], [15], [17], [18] used a batch fabrication procedure that would allow for integration of additional signal conditioning and control circuitry on the same substrate. In addition, our current multi-channel Neural probe chip is an improvement over our previously reported single-channel electrostatic microactuator [25]. We have improved the electrical interconnects to the individual moving microelectrodes using spring type leads that are integrated into the SUMMiTV process instead of the manual interconnects that had to be done post-fabrication in the electrostatic microactuator [25]. The spring type leads have almost no spring constant and, therefore, exert virtually no force on the microelectrodes as they are actuated. In addition, the electrical impedance offered by the spring-type leads is in the order of 10 kΩ, which does not compromise the single-neuronal monitoring capabilities of the polysilicon microelectrodes. The 3-channel Neural probe chip itself is of the same dimension (3 × 8 mm) as the single-channel electrostatic microactuator and microelectrode reported earlier. The thermal actuation mechanism offers several advantages over the electrostatic microactuation technology besides smaller footprint and, hence, higher packing density. With optimized packaging techniques, several of the current Neural probe chips can be easily stacked to realize 6-channel and 12-

channel microactuators and microelectrodes for a rodent brain. The thermal actuators are much more robust than the electrostatic microactuators and able to better withstand mechanical vibrations that occur during handling, and subsequently during behavior of the animal after implantation of the microelectrodes. The mechanical vibrations during the grooming routine of the rats were particularly very vigorous and the thermal actuators were able to withstand that without any adverse effects. The electrostatic microactuators were also quite sensitive to the alignment of the transmission gears with misalignment constituting a failure mode in the actuation. Fee and Leonardo have reported similar stalling issues with their micromotors [18]. In our current design, ratchet pawls have now replaced the transmission gears. We have not seen stalling problems in any of the five thermal microactuators tested so far.

The force generation capabilities of the thermal microactuators are three orders of magnitude higher than the electrostatic microactuator enabling easier passage of the microelectrode in the rodent brain. However, we have not yet tested if the microactuators are capable of penetrating the rodent dura mater with the microelectrode. We found that the thermal microactuators generated sufficient force to move the microelectrodes through the brain tissue. Our previous study using polysilicon microelectrodes without taper and a sensitive load cell [24] demonstrated forces in the order of 1 mN for the penetration of the dura, and drastically smaller forces required subsequently to move the microelectrode within the brain tissue. However, an earlier clinical study using spheres of 2.5-mm diameter moved at the rate of 0.33 mm/s [26] reported that the force experienced by the spheres to be in the range of 8 ± 2 g. Tuohy needles (17-gauge) moved at the rate of 20 mm/min have been found to require forces in the range of 5–8 N to puncture the dura mater [27]. The forces required to penetrate the dura and subsequently move the microelectrode within the brain vary widely depending on the size, geometry, and velocity of impact of the microelectrode at the time of penetration. Prior results from modeling studies have demonstrated that the thermal microactuators are capable of generating forces in the order of several hundreds of micro-Newtons [19]. If necessary, we can multiply the force generated by the microactuators by cascading multiple thermal microactuators for each microelectrode and synchronizing them. There is sufficient space on the chip to allow for an estimated maximum of four or five microactuators in cascade for each microelectrode. The thermal microactuators are also unaffected by changing humidity levels (likely to occur under long-term implantation) unlike the electrostatic microactuators.

We have used epoxy for the insulation of the polysilicon microelectrodes. However, more desirable alternatives like Parylene and silicon-nitride exist that have been proven to work well under chronic implantation conditions. In addition, silicon nitride as an insulator can be integrated into the SUMMiTV process thus allowing the Neural probe chip to retain its full microelectrode translation capability of 5 mm even after insulation. Future designs with silicon nitride insulation can, therefore, potentially enable monitoring single-neuronal activity of deeper subcortical and hippocampal neurons in the rodent brain.

Packaging remains a critical issue in long-term experiments involving single-neuronal monitoring. Smaller weight and dimensions that cause least hindrance to behavior and damage during implantation are always desirable. We have used standard packaging involving DIP sockets and external connectors for our current Neural probe chips resulting in overall dimensions of 15 × 25 mm and a weight of approximately 8 g. In contrast, the packaged miniature microdrive reported earlier [18] was 6 mm in diameter, 17 mm high, and weighed 1.5 g including the headstage amplifier. Our unpackaged Neural probe chip itself is approximately 3 × 8 mm and weighs only 34 mg approximately. The thermal microactuators occupy only approximately 3 × 1 mm area of the chip. The length of the chip is 8 mm primarily to accommodate the approximately 6 mm long microelectrodes and their associated spring-type leads for electrical contact as shown in Fig. 6(a) and (b). We are currently investigating customized ceramic and glass packaging options that promise to drastically reduce the overall

weight and width of the packaged Neural probe chip at the time of implantation. The current displacement resolution of the thermal microactuator is 8.8 μm compared to approximately 1 μm or less reported earlier by us [25] and Fee and Leonardo [18]. Having a smaller displacement resolution on the microactuator does enhance the ability to fine-tune the position of the microelectrode with respect to the neuron and can, therefore, improve the SNR in some cases. The displacement resolution of the thermal microactuators in our design can be enhanced quite readily by appropriate changes in the dimensions of the polysilicon strips that are thermally activated for actuation. In addition, several recording sites can be incorporated along the length of a single shank in future designs resulting in higher channel count.

V. Conclusion

In conclusion, a prototype Neural Probe chip that uses thermal microactuators to precisely position and reposition microelectrodes in the brain after implantation has been tested in preliminary experiments. The thermal microactuators and the microelectrodes need to be validated in a series of long-term experiments to identify failure modes, and to optimize packaging and insulation issues. After validation, the Neural probe chips have the potential of greatly enhancing our ability to interface with single neurons over long periods of time in-vivo by repositioning microelectrodes to a new location in case of breakdown in neuron-electrode interface due to a variety of mechanical and biological reasons. Repositioning of microelectrodes may also be desirable to monitor several functional locations sequentially with a single implanted microelectrode. In addition, the microactuated microelectrodes give us the flexibility of positioning the individual microelectrodes in an array at different depths enabling us to monitor neurons in different regions of the brain that are functionally related. Therefore, the Neural probe chip reported here promises to have significant impact on Neurophysiology research in memory, neuronal plasticity, repair and regeneration, motor learning and adaptation etc., where long-term monitoring of single neurons is critical to our understanding of neuronal function and dysfunction.

Jit Muthuswamy received the B. Tech. degree in electrical and electronic communication engineering from the Indian Institute of Technology, Kharagpur, India, in 1991. He received the M.S. and Ph.D. degrees in biomedical engineering in 1993 and 1996, respectively, and the MS degree in electrical engineering in 1996, all from Rensselaer Polytechnic Institute, Troy, NY.

He is currently an Assistant Professor with the Harrington Department of Bioengineering at Arizona State University, Tempe. His research interests are in BioMEMS and brain injury.

Murat Okandan received the B.S., M.S., and Ph.D. degrees in electrical engineering from the Pennsylvania State University, Philadelphia, in 1994, 1995 and 1998, respectively.
Since 1999, he has been with Sandia National Laboratories, Albuquerque, NM, where he is involved in microsystems technology and project development. His research interests include ultrathin gate dielectrics, enhanced micromachining technologies, and novel device concepts with applications in biological, medical, and sensing systems.

Aaron Gilletti received the B.S. and M.S. degree from the Harrington Department of Bioengineering at the Arizona State University, Tempe, in 2001 and 2003, respectively.
His research interests include BioMEMS technologies for neural interfaces and his thesis work involved BioMEMS for neuro-electrophysiology signal acquisition and the quantification of tissue micromotion.

Michael S. Baker received the M.S. degree in mechanical engineering from Brigham Young University, Provo, UT, in 2002.
He is currently a Senior Member of the Technical Staff in the MEMS Device Concepts department at Sandia National Laboratories, Albuquerque, NM. His research efforts are in the area of MEMS bistable mechanisms, compliant mechanism design, and actuation.

Tilak Jain received the B.Tech. degree in instrumentation engineering from the Indian Institute of Technology (IIT), Kharagpur, India, in 2002. He is currently a doctoral student in the Harrington Department of Bioengineering at Arizona State University, Tempe.
His research interests include BioMEMS technologies for neural interfaces, genetic engineering, and other biotechnological applications.

Acknowledgements

The authors would like to thank M. Shaw and the MDL staff for fabrication support.

References

1. BeMent SL, Wise KD, Anderson D, Najafi K, Drake KL. Solid state electrodes for multi channel multiplexed intracortical neuronal recording. IEEE Trans Biomed Eng 1986;BME-33:230–240. [PubMed: 3957372]
2. Charles, HK.; Massey, JT.; Mountcastle, VB. Polyimides as insulating layers for implantable electrodes. In: Mittal, KL., editor. Polyimides. 2. New York: Plenum; 1984. p. 1139-1155.
3. Eichenbaum H, Kuperstein M. Extracellular neural recording with multichannel microelectrodes. J Electrophysiol Tech 1986;13:189–209.
4. Kuperstein M, Whittington DA. A practical 24 channel microelectrode for neural recording *in vivo*. IEEE Trans Biomed Eng 1981;BME-28:288–293. [PubMed: 6262216]
5. Pickard RS. A review of printed circuit microelectrodes and their production. J Neurosci Methods 1979;1:301–319. [PubMed: 544973]
6. Pochay P, Wise KD, Allard LF, Rutledge LT. A multichannel depth probe fabricated using electron beam lithography. IEEE Trans Biomed Eng 1979;BME-26:199–206. [PubMed: 437800]
7. Prohaska O, Pacha F, Pfundner P, Petsche H. A 16-fold semi-microelectrode for intracortical recording of field potentials. Electrenceph Clin Neurophysiol 1979;47:629–631.
8. Wise KD, Angell JB, Starr A. An integrated circuit approach to extracellular microelectrodes. IEEE Trans Biomed Eng 1970;BME-17:238–246. [PubMed: 5431636]
9. Blum NA, Carkhuff BG, Charles HK, Edwards RL, Meyer RA. Multisite microprobes for neural recordings. IEEE Trans Biomed Eng Jan 1991;38(1):p. 68.
10. Normann, RA.; Campbell, PK.; Li, WP. Annu Int Conf IEEE Engineering in Medicine and Biology Society. 2. New Orleans, LA: 1988. Silicon based microstructures suitable for intracortical electrical stimulation; p. 714-715.
11. Eckhorn R, Thomas U. A new method for the insertion of multiple microprobes into neural and muscular tissue, including fiber electrodes, fine wires, needles and microsensors. J Neurosci Methods 1993;49:175–179. [PubMed: 8271837]
12. Mountcastle VB, Reitboeck HJ, Poggio GF, Steinmetz MA. Adaptation of the Reitboeck method of multiple microelectrode recording to the neocortex of the waking monkey. J Neurosci Methods 1991;36:77–84. [PubMed: 2062112]
13. Reitboeck HJ. A 19-channel matrix drive with individually controllable fiber microelectrodes for neurophysiological applications. IEEE Trans Syst Man Cybern 1983;SMC-113:626–683.
14. Reitboeck HJ, Werner G. Multi-electrode recording system for the study of spatio-temporal activity patterns of neurons in the central nervous system. Experientia 1983;39:339–341. [PubMed: 6825809]
15. Wilson MA, McNaughton BL. Dynamics of the hippocampal ensemble code for space. Science 1993;261:1055–1058. [PubMed: 8351520]
16. ——— Reactivation of the hippocampal ensemble memories during sleep. Science 1994;265:676–679. [PubMed: 8036517]
17. Wilson FAW, Ma YY, Greenberg PA, Ryou JW, Kim BH. A microelectrode drive for long term recording of neurons in freely moving and chaired monkeys. J Neurosci Methods 2003;127:49–61. [PubMed: 12865148]
18. Fee MS, Leonardo A. Miniature motorized microdrive and commutator system for chronic neural recording in small animals. J Neurosci Methods 2001;112:83–94. [PubMed: 11716944]
19. Plass RA, Baker MS, Walraven JA. Electrothermal actuator reliability studies. Proc SPIE 2004;5343:15–21.
20. Cragun, R.; Howell, LL. Linear thermomechanical microactuators. presented at the ASME International Mechanical Engineering Congress and Exposition; Nashville, TN. 1999.
21. Que L, Park JS, Gianchandani YB. Bent-beam electrothermal actuators—part I: single beam and cascaded devices. J Micromech Syst 2001;10:247–254.
22. Lott CD, McLain TW, Harb JN, Howell LL. Modeling the thermal behavior of a surface-micromachined linear-displacement thermomechanical microactuator. Sensors Actuators A—Physical 2002;101:239–250.

23. Sniegowski JJ, Boer MPD. IC-compatible polysilicon surface micromachining. Annu Rev Mater Sci 2000;30:299–333.

24. Muthuswamy J, Okandan M, Jackson N. Single neuronal recordings using surface micro-machined polysilicon microelectrodes. J Neurosci Methods 2005;142(1):45–54. [PubMed: 15652616]

25. Muthuswamy J, Okandan M, Jain T. Electrostatic microactuators for precise positioning of neural microelectrodes. IEEE Trans Biomed Eng. 2005to be published

26. Howard MA, Abkes BA, Ollendieck MC, Noh MD, Ritter RC, Gillies GT. Measurement of the force required to move a neurosurgical probe through *in vivo* human brain tissue. IEEE Trans Biomed Eng Jul 1999;46(7):891–894. [PubMed: 10396907]

27. Lewis MC, Lafferty JP, Sacks MS, Pallares VS, TerRiet M. How much work is required to puncture dura with Tuohy needles? Br J Anaesth 2000;85:238–241. [PubMed: 10992831]

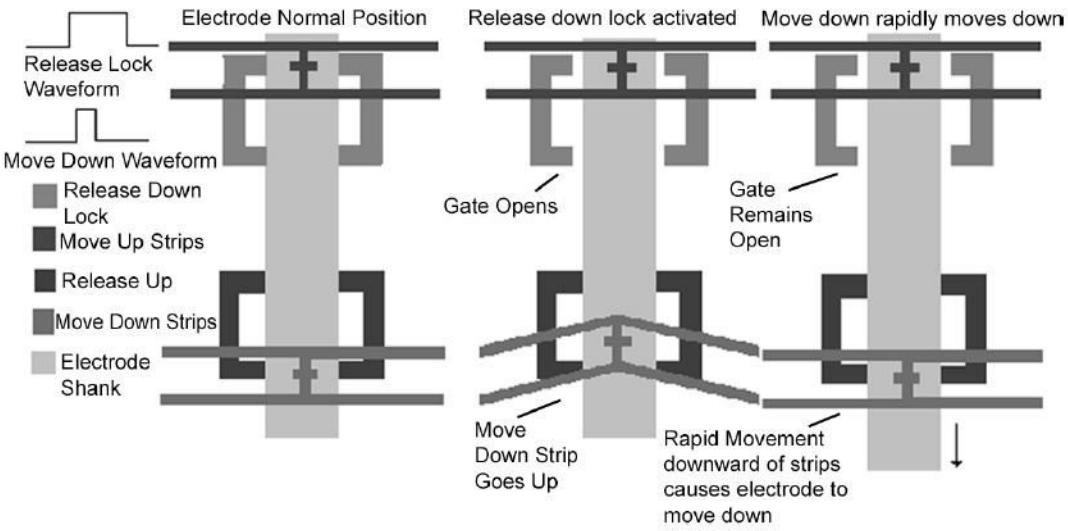

Fig. 1.

Principle of thermal actuation—slightly angled pair of polysilicon strips on either side of a polysilicon shuttle in the center expand in plane upon heating and move the shuttle down. In our design, two such thermal actuators were used to achieve up and down motion of the shuttle, respectively. In addition, four more thermal actuators (two on either side of the shuttle) were used to engage and disengage locks during motion in either direction. The locks remain engaged in the inactive state and were disengaged only when the actuators controlling the locks were activated. Two actuators were dedicated to release the up-lock and two to release the down-lock upon activation.

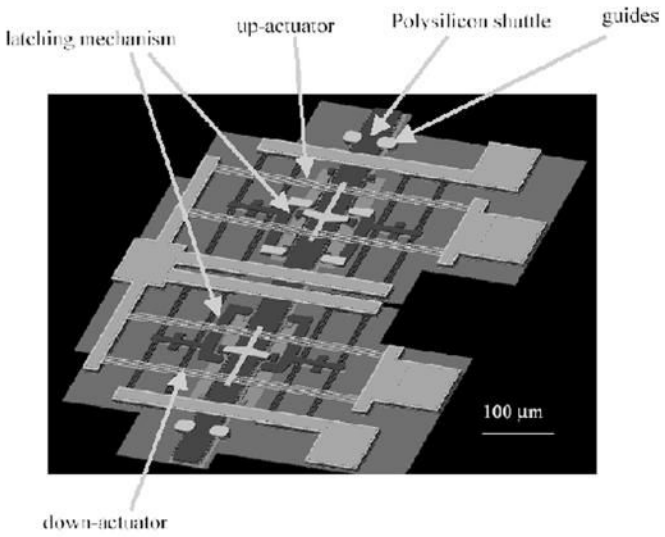

Fig. 2.
Computer-aided design layout of one of the polysilicon microelectrode (shown in dark grey running down the middle of the layout) and associated thermal microactuators. The contact pads are shown in light grey.

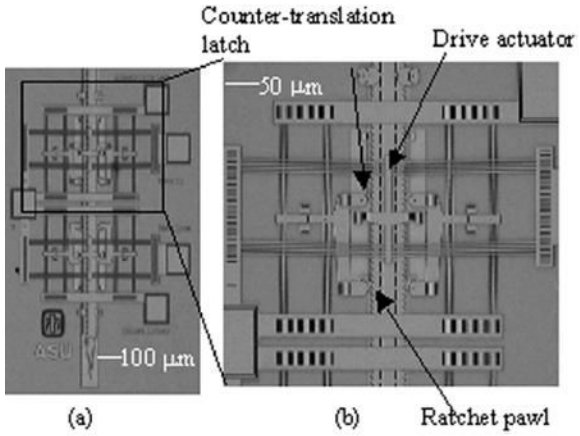

Fig. 3.

Micrographs of (a) complete drive mechanism and (b) zoomed view of the top half of the actuator. The 5 bond pads (move up, move down, actuator-up lock, actuator-down lock and ground pads) that are used to energize the microactuator are visible in (a). The counter-translation latch and ratchet pawl are engaged in a lock position in (b).

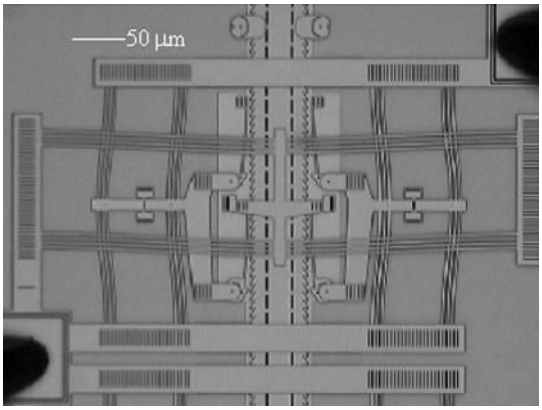

Fig. 4.
Micrograph showing two thermal actuators energized to pull and release the counter-translation latches and ratchet pawls on either side of the microelectrode (shuttle) to disengage them and allow translation of the microelectrode in the downward direction.

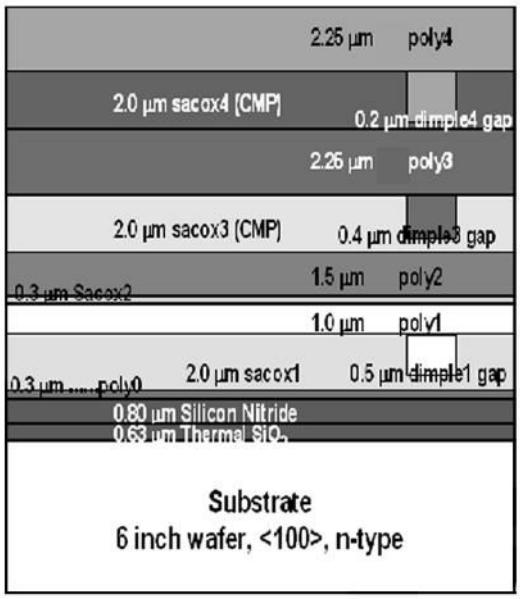

Fig. 5.
Schematic of the SUMMiTV process indicating the different layers of polysilicon available for fabricating mechanical and electrical components.

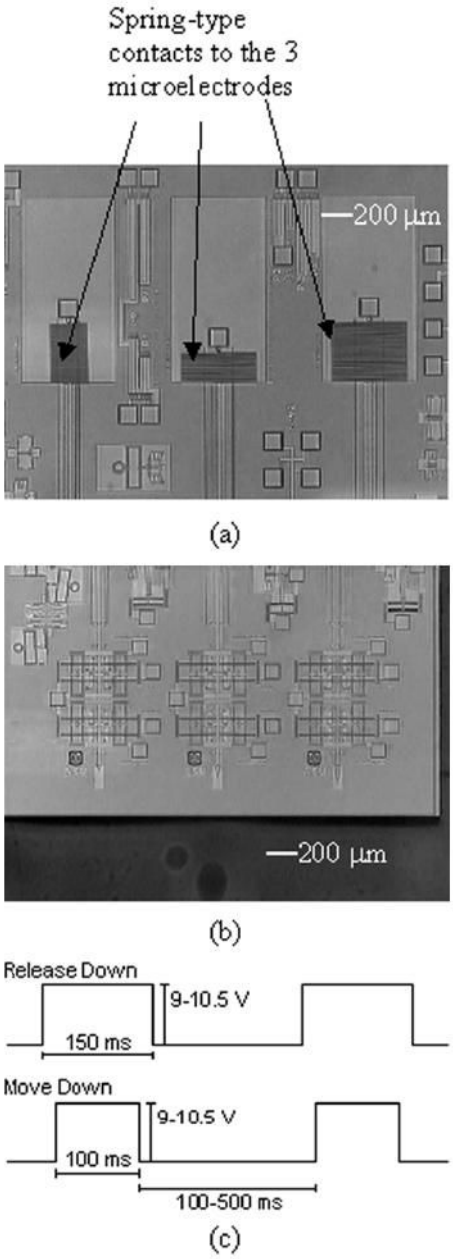

Fig. 6.

(a). Spring-type leads make electrical contact from stationary bond pads to the top of the moving microelectrodes. The springs-type leads are either 1.6 mm or 3.2 mm long and have no spring constant to mechanically retract the microelectrode. They just make electrical contact with a resistance of approximately 10 kΩ. (b). A close-up of the bottom edge of the 3-channel neural probe chip showing the three adjacent microactuators and associated microelectrodes poised to extend out of the chip. The microelectrodes are separated by approximately 800 μm. (c). Typical waveforms used to drive the thermal actuator probe. Voltage level is specific to each chip and the pulse duration and latency is dependent on the desired speed for driving the device.

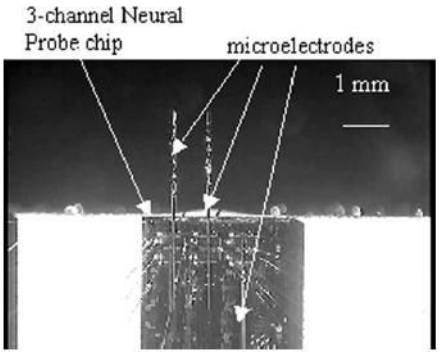

Fig. 7.

A photograph of the 3-channel neural probe chip showing the end with two of the microelectrodes extended over the edge of the chip and the third microelectrode in the retracted position within the chip. The microelectrodes are epoxy insulated and separated by approximately 800 μm to minimize cross-channel electrical coupling. The chip is mounted on a standard DIP socket covered by glass slide to protect the microactuators and also to allow for visualization after implantation. The whole packaging weighs approximately 8.14 g and is suitable for chronic implantation on a rat head.

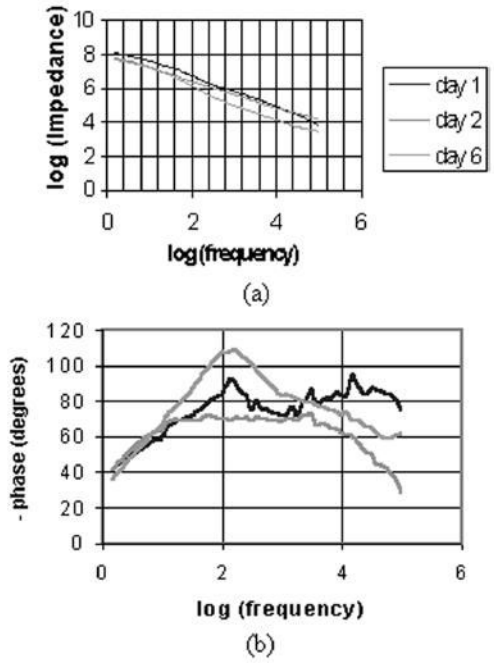

Fig. 8.

Impedance [magnitude in (a) and phase in (b)] spectra of epoxy-coated polysilicon microelectrodes dipped in phosphate buffered saline over a period of 6 days indicate stability in the impedance magnitude of the polysilicon-epoxy interface.

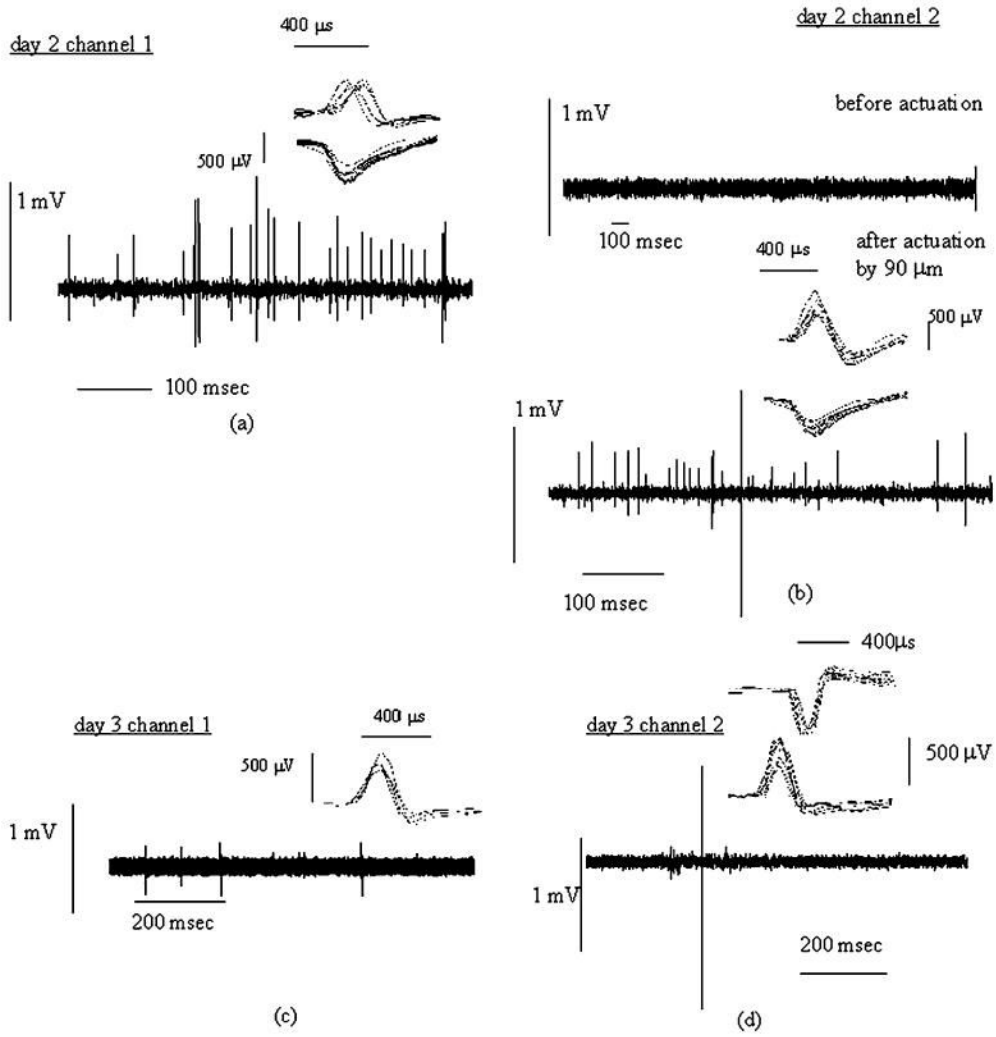

Fig. 9.

Multi-unit activity using the thermal microactuators over a period of 3 days (a) from channel 1 on day 2 and (b) from channel 2 on day 2. Multi-unit data after actuation by approximately 90 μm is also shown in (b). Data from (c) channel 1 on day 3 shows subdued neuronal activity with only one single unit in the inset and (d) channel 2 on day 3. The insets display multiple occurrences of single unit activity after sorting.